Hydrazone chelators for the treatment of iron overload disorders: iron coordination chemistry and biological activity — Source link ⧉

Paul V. Bernhardt, Piao Chin, Philip C. Sharpe, Des R. Richardson

Institutions: University of Queensland, University of Sydney

Related papers:

- A short history of SHELX

- Structural Variations and Formation Constants of First-Row Transition Metal Complexes of Biologically Active Aroylhydrazones

- Cytotoxic iron chelators: characterization of the structure, solution chemistry and redox activity of ligands and iron complexes of the di-2-pyridyl ketone isonicotinoyl hydrazone (HPKIH) analogues

- The Evolution of Iron Chelators for the Treatment of Iron Overload Disease and Cancer

- ORTEP-3 for Windows - a version of ORTEP-III with a Graphical User Interface (GUI)

Dalton Transactions

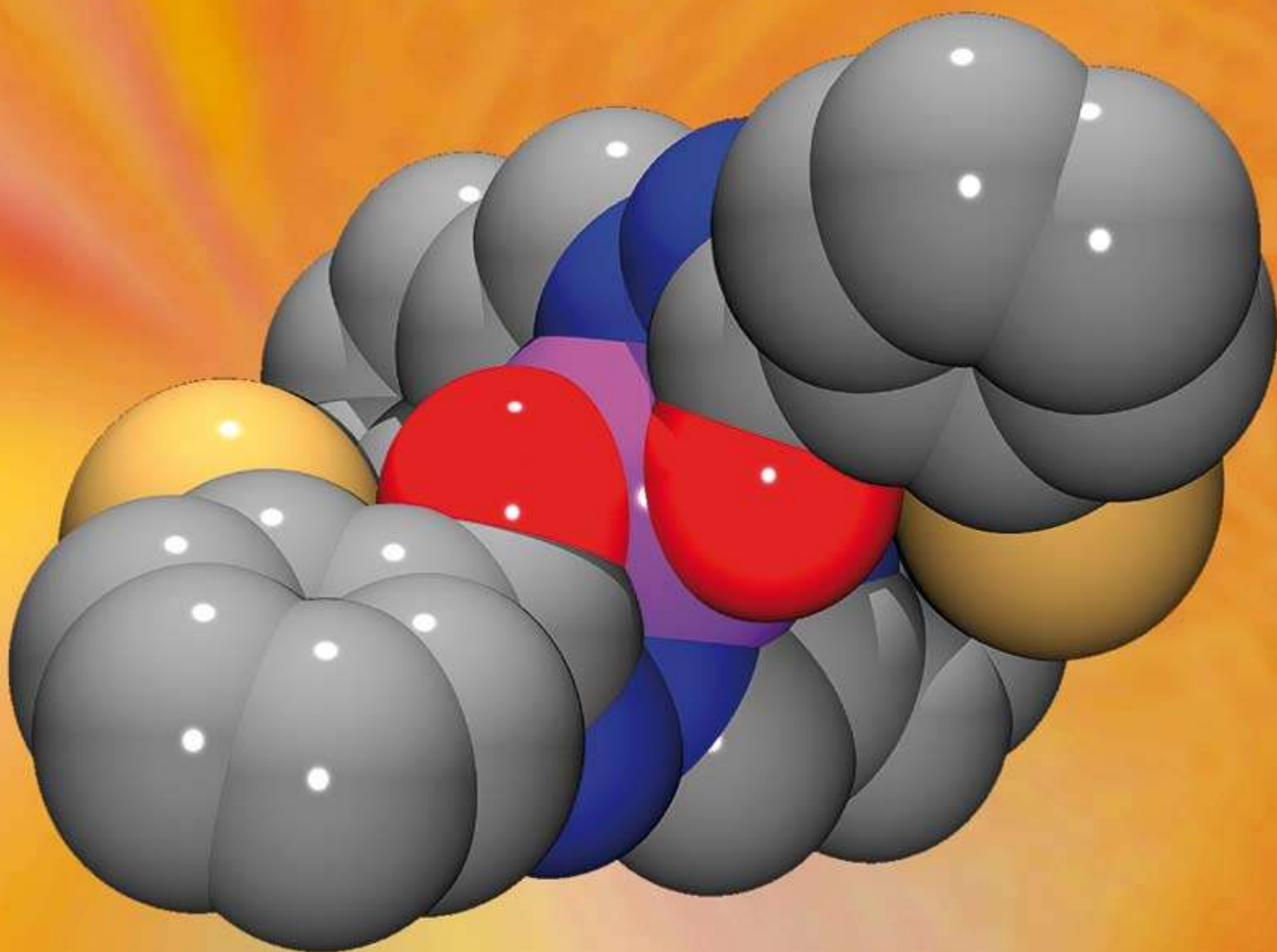**HOT ARTICLE**
Paul V. Bernhardt *et al*.
Hydrazone chelators for the
treatment of iron overload disorders:
iron coordination chemistry and
biological activity

PERSPECTIVE
Paul V. Bernhardt
Coordination chemistry and biology
of chelators for the treatment of iron
overload disorders

RSCPublishing

1477-9226(2007)30;1-7

Hydrazone chelators for the treatment of iron overload disorders: iron coordination chemistry and biological activity†

Paul V. Bernhardt,*[a] Piao Chin,[a] Philip C. Sharpe[a] and Des R. Richardson*[b]

The potentially tridentate ligand 2-pyridinecarbaldehyde isonicotinoyl hydrazone (HPCIH) and its analogues are an emerging class of orally effective Fe chelators that show great promise for the treatment of Fe overload diseases. Herein, we present an extensive study of the Fe coordination chemistry of the HPCIH analogues including the first crystallographically characterised Fe^{II} complex of these chelators. Unlike most other clinically effective Fe chelators, the HPCIH analogues bind Fe^{II} and not Fe^{III}. In fact, these chelators form low-spin bis-ligand Fe^{II} complexes, although NMR suggests that the complexes are close to the high-spin/low-spin crossover. All the Fe complexes show a high potential $Fe^{III/II}$ redox couple (> 500 mV vs. NHE) and cyclic voltammetry in aqueous or mixed aqueous/organic solvents is irreversible as a consequence of a rapid hydration reaction that occurs upon oxidation. A number of the HPCIH analogues show high activity at inducing Fe efflux from cells and also at preventing Fe uptake by cells from the serum Fe transport protein transferrin. As a class of ligands, these chelators are more effective at reducing Fe uptake from transferrin than inducing Fe mobilisation from cells. This may be related to their ability to intercept Fe^{II} after its release from transferrin within the cell. Our studies indicate that their Fe chelation efficacy is due, at least in part, to the fact that these ligands and their Fe^{II} complexes are neutral at physiological pH (7.4) and sufficiently lipophilic to permeate cell membranes.

Introduction

Under normal circumstances in mammals, only trace levels of Fe exist outside its physiological sinks i.e. transferrin, ferritin, heme, iron–sulfur clusters etc., where it is constantly shuttled between storage and reuse.[1,2] Excess Fe, particularly when it is uncomplexed, can catalyse the generation of harmful reactive oxygen species (ROS) through Fenton chemistry.[3] Thus, cellular Fe homeostasis is a crucial function. Humans are especially susceptible to Fe overload as they have no natural mechanism for Fe excretion.[4,5] Irrespective of the cause of Fe overload (e.g. chronic blood transfusions in the treatment of β-thalassemia, Friedreich's ataxia etc.), the ROS that ensue from Fe-mediated redox reactions damage membranes, proteins and DNA, leading to pathology.[1] Sufferers of Fe overload must then undergo chelation therapy to facilitate Fe excretion.[1]

For many years, the only Fe-chelating drug that was approved and widely utilised world-wide for the treatment of Fe overload was desferrioxamine B (DFO or desferal), a tri-hydroxamic acid which possesses high specificity for Fe^{III} (Fig. 1).[1]

Unfortunately, the use of DFO suffers from serious problems, including: (i) its high cost, making it unaffordable for patients in developing countries, where the incidence of β-thalassemia major
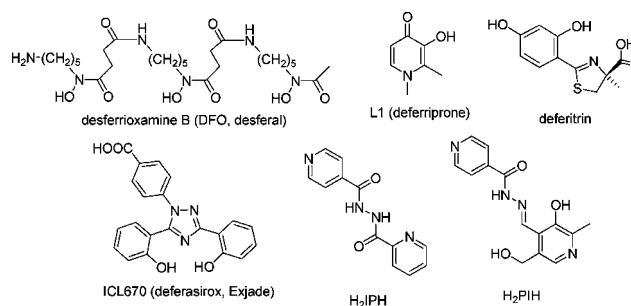
[a]Centre for Metals in Biology, Department of Chemistry, University of Queensland, Brisbane, 4072, Australia. E-mail: P.Bernhardt@uq.edu.au
[b]Iron Metabolism and Chelation Program, Department of Pathology and Bosch Institute, University of Sydney, Sydney, 2006, Australia. E-mail: d.richardson@med.usyd.edu.au

† CCDC reference numbers 640839–640845. For crystallographic data in CIF or other electronic format see DOI: 10.1039/b704102k

Fig. 1 Biologically active Fe chelators.

is greatest, (ii) it is poorly absorbed via the oral route[6] and does not readily access intracellular pools due to its hydrophilicity;[7] and (iii) DFO is rapidly metabolised, necessitating prolonged subcutaneous infusions (12–24 h day^{-1}, 5–6 times week^{-1}) leading to poor compliance.[1,8] DFO is also ineffective at mobilising Fe from Fe-loaded mitochondria,[9–11] rendering it unsuitable for the treatment of the neuro- and cardio-degenerative disease, Friedreich's ataxia.

Deferiprone (1,2-dimethyl-3-hydroxypyridin-4-one), also known as L1 (Fig. 1), is moderately effective as an orally-active Fe chelator.[1] However, the clinical use of deferiprone has a controversial history and is still not approved world-wide.[12] Recently, the chelator ICL670A (deferasirox or Exjade, Fig. 1) has been approved for clinical use in Europe, USA, Canada and Australia as an orally-active Fe chelator. ICL670A is the most promising and advanced alternative to DFO that may be given either as an oral suspension or in capsule form.[13,14] Another

potentially orally-active chelator, deferitrin (Fig. 1), has recently completed a Phase I human trial.[15]

Our interest is in the development of chelators based on 2-pyridinecarbaldehyde isonicotinoyl hydrazone (HPCIH, Fig. 2) that show high Fe chelation efficacy in cell culture models and are orally effective in mice.[16–18] All analogues bear the 2-pyridinecarbaldehyde hydrazone backbone, which comprises pyridine-N, imine-N and carbonyl-O donor atoms forming a meridionally coordinating tridentate ligand (Fig. 2). A number of HPCIH analogues have been synthesized to create a series with varying physicochemical properties, such as lipophilicity and ionisation constants.[16,19] Given the high activity that some HPCIH analogues have shown *in vitro*[11,16] and *in vivo*,[18] an investigation of their physicochemical properties and Fe coordination chemistry is clearly warranted.
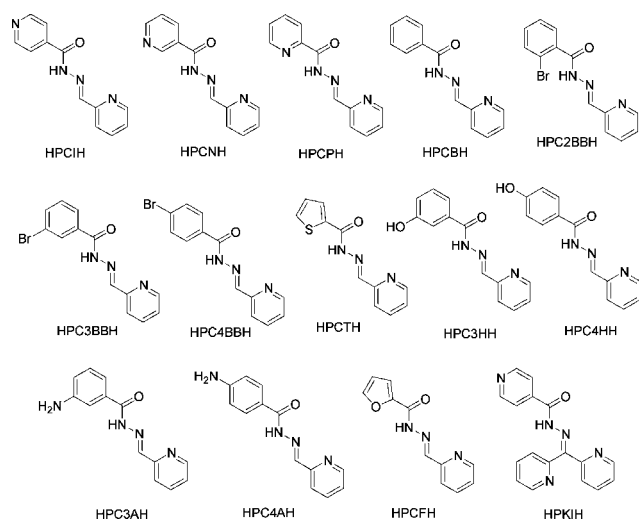

Fig. 2 The HPCIH analogues and the related hydrazone HPKIH.

Previously, we showed that the parent compound of the series, HPCIH, was oxidised in aerated aqueous solution in the presence of Fe to afford *N*-(isonicotinoyl)-*N′*-(picolinoyl)hydrazine (H₂IPH, Fig. 1).[20] Interestingly, other closely related ligands of this series (*e.g.* 2-pyridinecarbaldehyde (4′-aminobenzoyl)hydrazone; HPCAH) did not undergo oxidation in the presence of Fe(II) or Fe(III), suggesting it was a reaction unique to HPCIH.[19] However, isolation and characterisation of Fe^{II} complexes from the HPCIH series has been challenging, in contrast to the facile isolation and crystallographic characterisation of a number of other divalent first row transition metal complexes of HPCIH and HPC4AH (Mn, Co, Ni, Cu and Zn).[19]

Here we report the first comprehensive investigation of the HPCIH analogues and their Fe^{II} complexes. Moreover, we have synthesized a number of novel HPCIH chelators which are isomeric with other chelators from this family that have demonstrated activity in the past (*e.g.* HPCNH, HPCPH, HPC2BBH, HPC3BBH, Fig. 2). From these studies, we define important structure–activity relationships of the HPCIH analogues that should be noted for the design of future chelators for clinical use.

Experimental

Syntheses

All commercially available chemicals and solvents used in this work were of analytical grade. Desferal™ (DFO) was from Novartis, Summit, NJ, USA.

Free ligands

The hydrazones were prepared *via* Schiff base condensation.[16,19] Recrystallisation from aqueous EtOH afforded pure ligand in >80% yield. Spectroscopic data for HPCIH and HPC4AH (formerly referred to as HPCAH) have been reported[19] and only results for the new ligands are included below. Slow evaporation of aqueous methanol (1 : 1) solutions of the ligands afforded crystals suitable for X-ray work.

The hydrogen perchlorate salts [H₂PC3BBH]ClO₄·2H₂O and [H₂PC4BBH]ClO₄·H₂O were crystallised from aqueous solutions acidified to pH 2 with HClO₄. The crystals that formed were suitable for X-ray work and these were filtered off and air dried.

2-Pyridinecarbaldehyde nicotinoyl hydrazone (HPCNH·2H₂O). Anal. found C, 55.04 H, 5.43; N, 21.35%; calculated for C₁₂H₁₄N₄O₃: C, 54.96; H, 5.38; N, 21.36%. IR: $\tilde{\nu}_{CO}$ 1662 cm⁻¹. ¹H NMR (DMSO-d_6): δ = 7.43 (t, 1H), 7.58 (q, 1H), 7.94 (m, 2H), 8.22 (d, 1H), 8.48 (s, 1H), 8.62 (d, 1H), 8.78 (d, 1H), 9.10 (d, 1H) and 12.23 (s, 1H). ¹H NMR (methanol-d_4): δ = 7.46 (t, 1H), 7.62 (q, 1H), 7.91 (t, 1H), 8.27 (d, 1H), 8.38 (d, 1H), 8.43 (s, 1H), 8.59 (d, 1H), 8.78 (d, 1H) and 9.14 (d, 1H). ¹³C NMR (DMSO-d_6): δ = 120.3, 123.9, 124.8, 129.2, 135.8, 137.2, 148.9, 149.8, 152.7, 153.2 and 162.2. ¹³C NMR (methanol-d_4): δ = 122.4, 125.3, 126.2, 130.3, 137.6, 138.6, 149.6, 150.1, 150.2, 153 4, 154.2 and 164.9 ppm.

2-Pyridinecarbaldehyde picolinoyl hydrazone (HPCPH). Anal. found C, 63.82; H, 4.39; N, 24.93%; calculated for C₁₂H₁₀N₄O: C, 63.71; H, 4.46; N, 24.76%. IR: $\tilde{\nu}_{CO}$ 1698 cm⁻¹. ¹H NMR (DMSO-d_6): δ = 7.41 (m, 1H), 7.67 (m, 1H), 7.90 (t, 1H), 8.10 (m, 3H), 8.62 (d, 2H), 8.70 (s, 1H) and 12.51 (s, 1H). ¹H NMR (methanol-d_4): δ = 7.48 (t, 1H), 7.66 (t, 1H), 8.00 (m, 3H), 8.28 (m, 2H), 8.56 (s, 1H), 8.61 (d, 1H) and 8.75 (d, 1H). ¹³C NMR (DMSO-d_6): δ = 120.3, 123.1, 124.7, 127.4, 137.1, 138.3, 148.8, 149.6, 149.7, 153.6 and 161.1. ¹³C NMR (methanol-d_4): δ = 122.4, 124.1, 126.1, 128.4, 138.6, 138.9, 150.0, 150.2, 150.4, 154.5 and 163.7 ppm.

2-Pyridinecarbaldehyde benzoyl hydrazone (HPCBH·H₂O). Anal. found C, 64.00; H, 5.31; N, 17.08%; calculated for C₁₃H₁₃N₃O₂: C, 64.19; H, 5.39; N, 17.29%. IR: $\tilde{\nu}_{CO}$ 1658 cm⁻¹. ¹H NMR (DMSO-d_6): δ = 7.53 (m, 4H), 7.92 (m, 4H), 8.50 (s, 1H), 8.61 (d, 1H) and 12.09 (s, 1H). ¹H NMR (methanol-d_4): δ = 7.56 (m, 4H), 7.96 (m, 3H), 8.32 (d, 1H), 8.44 (s, 1H) and 8.60 (d, 1H). ¹³C NMR (DMSO-d_6): δ = 120.1, 124.6, 128.0, 128.8, 132.2, 133.4, 137.1, 148.3, 149.8, 153.5 and 163.7. ¹³C NMR (methanol-d_4): δ = 122.3, 126.0, 128.9, 129.8, 133.6, 133.8, 138.6, 149.4, 150.2, 154.5 and 167.3 ppm.

2-Pyridinecarbaldehyde-3′-aminobenzoyl hydrazone (HPC3AH). Anal. found C, 65.14; H, 5.13; N, 23.18%; calculated for C₁₃H₁₂N₄O: C, 64.99; H, 5.03; N, 23.32%. IR: $\tilde{\nu}_{CO}$ 1661 cm⁻¹. ¹H NMR (DMSO-d_6): δ = 5.39 (s, 2H), 6.77 (d, 1H), 7.12 (m, 3H), 7.39 (t, 1H), 7.90 (m, 2H), 8.47 (s, 1H), 8.61 (d, 1H) and 11.94 (s,

1H). ^{13}C NMR (DMSO-d_6): δ = 113.2, 114.9, 117.4, 120.0, 124.5, 129.2, 134.3, 137.1, 147.8, 149.2, 149.8, 153.7 and 164.4 ppm.

2-Pyridinecarbaldehyde-4′-bromobenzoyl hydrazone (HPC-4BBH·H$_2$O). Anal. found C, 48.72; H, 3.62; N, 13.10%; calculated for C$_{13}$H$_{12}$BrN$_3$O$_2$: C, 48.47; H, 3.75; N, 13.04%. IR: $\tilde{v}_{CO}$ 1666 cm^{-1}. ^{1}H NMR (DMSO-d_6): δ = 7.38 (t, 1H), 7.85 (m, 6H), 8.47 (s, 1H), 8.59 (d, 1H) and 12.20 (s, 1H). ^{1}H NMR (methanol-d_4): δ = 7.48 (t, 1H), 7.73 (d, 2H), 7.94 (m, 3H), 8.34 (d, 1H), 8.43 (s, 1H) and 8.63 (d, 1H). ^{13}C NMR (DMSO-d_6): δ = 120.2, 124.7, 126.0, 130.1, 131.8, 132.4, 137.1, 148.6, 149.7, 153.4 and 162.7 ppm.

2-Pyridinecarbaldehyde-3′-bromobenzoyl hydrazone (HPC-3BBH·H$_2$O). Anal. found C, 48.74; H, 3.60; N, 13.05%; calculated for C$_{13}$H$_{12}$BrN$_3$O$_2$: C, 48.47; H, 3.75; N, 13.04%. IR:$\tilde{v}_{CO}$ 1662 cm^{-1}. ^{1}H NMR (DMSO-d_6): δ = 7.41 (t, 1H), 7.50 (t, 1H), 7.80 (d, 1H), 7.88 (t, 1H), 7.92 (d, 1H), 7.98 (d, 1H), 8.10 (s, 1H), 8.46 (s, 1H) and 8.61 (d, 1H). ^{13}C NMR (DMSO-d_6): δ = 120.0, 121.8, 124.5, 127.0, 130.2, 130.8, 134.7, 135.3, 136.9, 148.6, 149.6, 153.1 and 161.9 ppm.

2-Pyridinecarbaldehyde-2′-bromobenzoyl hydrazone (HPC-2BBH). Anal. found C, 51.72; H, 3.36; N, 14.20%; calculated for C$_{13}$H$_{10}$BrN$_3$O: C, 51.34; H, 3.31; N, 13.82%. IR: $\tilde{v}_{CO}$ 1671 cm^{-1}. ^{1}H NMR (DMSO-d_6): δ = 7.44 (m, 4H), 7.73 (t, 1H), 7.93 (m, 2H), 8.31 (s, 1H), 8.60 (m, 1H) and 12.15 (s, 1H). ^{1}H NMR (methanol-d_4): δ = 7.47 (m, 4H), 7.60 (d, 1H), 7.92 (t, 1H), 8.24 (s, 1H), 8.29 (d, 1H) and 8.58 (d, 1H). ^{13}C NMR (DMSOd_6): δ = 120.5, 122.6, 126.6, 129.3, 130.5, 133.5, 134.3, 137.1, 139.0, 149.7, 150.6, 153.2 and 166.3 ppm.

2-Pyridinecarbaldehyde-4′-hydroxybenzoyl hydrazone (HPC-4HH). Anal. found C, 64.64; H, 4.61; N, 17.52%; calculated for C$_{13}$H$_{11}$N$_3$O$_2$: C, 64.72; H, 4.60; N, 17.42%. IR: $\tilde{v}_{CO}$ 1648 cm^{-1}. ^{1}H NMR (DMSO-d_6): δ = 6.88 (d, 2H), 7.39 (m, 1H), 7.83 (d, 2H), 7.92 (t, 2H), 8.45 (s, 1H), 8.60 (d, 1H), 10.19 (s, 1H) and 11.86 (s, 1H). ^{1}H NMR (methanol-d_4): δ = 6.95 (d, 2H), 7.46 (t, 1H), 7.93 (m, 3H), 8.33 (d, 1H), 8.41 (s, 1H) and 8.59 (d, 1H). ^{13}C NMR (DMSO-d_6): δ = 115.3, 120.0, 123.8, 124.4, 130.1 (br), 137.0, 147.3 (br), 149.7, 153.7, 161.1 and 163.2 (br). ^{13}C NMR (methanol-d_4): δ = 116.4, 122.2, 124.3, 125.9, 131.1, 138.6, 148.4, 150.1, 154.7 and 163.1 ppm.

2-Pyridinecarbaldehyde-3′-hydroxybenzoyl hydrazone (HPC-3HH). Anal. found C, 64.61; H, 4.60; N, 17.20%; calculated for C$_{13}$H$_{11}$N$_3$O$_2$: C, 64.72; H, 4.60; N, 17.42%. ^{1}H NMR (DMSO-d_6): δ = 7.01 (m, 1H), 7.38 (m, 4H), 7.90 (m, 2H), 8.49 (s, 1H), 8.60 (d, 1H), 9.82 (s, 1H) and 12.01 (s, 1H). ^{13}C NMR (DMSO-d_6): δ = 114.8, 118.5, 119.2, 120.1, 124.6, 129.8, 134.8, 137.1, 148.2, 149.7, 153.6, 157.7 and 163.7 ppm.

2-Pyridinecarbaldehyde-2′-thienyl hydrazone (HPCTH·H$_2$O). Anal. found C, 52.84; H, 4.36; N, 16.87%; calculated for C$_{11}$H$_{11}$N$_3$O$_2$S: C, 53.00; H, 4.45; N, 16.86%. IR: $\tilde{v}_{CO}$ 1632 cm^{-1}. ^{1}H NMR (DMSO-d_6): δ = 7.24 (t, 1H), 7.42 (m, 1H), 7.95 (br, m, 5H), 8.63 (d, 1H) and 12.06 (s, 1H). ^{13}C NMR (DMSO-d_6): δ = 120.3, 124.6, 127.1 (br), 128.4 (br), 129.6 (br), 132.5 (br), 132.9 (br), 135.3 (br), 137.2 (br), 138.1 (br), 144.7 (br), 147.9 (br), 149.8, 153.3, 158.1 (br) and 161.8 (br) ppm.

2-Pyridinecarbaldehyde-2′-furoyl hydrazone (HPCFH·H$_2$O). Anal. found C, 56.69; H, 4.76; N, 17.91%; calculated for C$_{11}$H$_{11}$N$_3$O$_3$: C, 56.65; H, 4.75; N, 18.02%. IR: $\tilde{v}_{CO}$ 1661 cm^{-1}. ^{1}H NMR (methanol-d_4): δ = 6.69 (q, 1H), 7.38 (d, 1H), 7.44 (t, 1H), 7.80 (d, 1H), 7.93 (t, 1H), 8.28 (d, 1H), 8.43 (s, 1H) and 8.58 (d, 1H). ^{13}C NMR (methanol-d_4): δ = 113.3, 117.6, 122.2, 126.0, 138.6, 147.4, 147.5, 149.5, 150.1, 154.4 and 157.6 ppm.

Fe complexes (general synthesis)

The free ligand (4 mmol) was dissolved in 40 cm^3 of MeCN and 32 mmol of triethylamine and the mixture purged with nitrogen. Then 1.6 mmol of Fe(ClO$_4$)$_2$·6H$_2$O was dissolved in 10 cm^3 of oxygen-free MeCN and added drop-wise to the basic ligand solution with stirring under nitrogen. The mixture was subsequently refluxed under nitrogen for 3 h. The green Fe^{II} complex was filtered off, while the mixture was hot and washed with methanol and acetone. The products were usually of high purity and no re-crystallisation was necessary unless stated. Yields: 75–95%.

[Fe(PCIH)$_2$]·1/2H$_2$O. Anal. found: C, 55.42; H, 3.44; N, 21.79%; calculated for C$_{24}$H$_{19}$FeN$_8$O$_{2.5}$: C, 55.94; H, 3.72; N, 21.74%. IR: $\tilde{v}_{max}$ (most intense peak) 1362 cm^{-1}. Electronic spectrum (MeOH): λ_{max}, nm (ε, dm^3 mol^{-1} cm^{-1}) 649 (4000), 349 (39 000), 268 (19 500), 229 (35 200). ^{1}H NMR (d_6-DMSO): δ = 10.33 (s, 2H), 10.79 (s, 2H), 13.69 (s, 1H), 15.09 (s, 1H), 19.75 (s, 1H) ppm.

Fe(PCNH)$_2$. Anal. found: C, 56.94; H, 3.59; N, 22.27%; calculated for C$_{24}$H$_{18}$FeN$_8$O$_2$: C, 56.93; H, 3.58; N, 22.13%. IR: $\tilde{v}_{max}$ (most intense peak) 1363 cm^{-1}. Electronic spectrum (MeOH): λ_{max}, nm (ε, dm^3 mol^{-1} cm^{-1}) 642 (3190), 348 (32 900), 270 sh ($\sim$ 18 000), 240 (26 800). ^{1}H NMR (d_6-DMSO): δ = 9.60 (s, 1H), 9.74 (s, 1H), 10.65 (s, 1H), 11.86 (s, 1H), 13.86 (s, 1H), 15.61 (s, 1H), 20.31 (s, 1H) ppm.

[Fe(PCBH)$_2$]·1/2H$_2$O. Anal. found: C, 60.90; H, 3.90; N, 16.36%; calculated for C$_{26}$H$_{21}$FeN$_6$O$_{2.5}$: C, 60.83; H, 4.12; N, 16.37%. IR: $\tilde{v}_{max}$ (most intense peak) 1358 cm^{-1}. Electronic spectrum (MeOH): λ_{max}, nm (ε, dm^3 mol^{-1} cm^{-1}) 637 (3170), 348 (30 500), 256 (22 700). ^{1}H NMR (d_6-DMSO): δ = 8.38 (s, 1H), 9.25 (s, 2H), 9.80 (s, 2H), 12.03 (s, 1H), 13.77 (s, 1H), 16.62 (s, 1H) ppm.

[Fe(PC4AH)$_2$]·21/2H$_2$O. Anal. found: C, 54.08; H, 4.26; N, 19.34%; calculated for C$_{26}$H$_{27}$FeN$_8$O$_{4.5}$: C, 53.90; H, 4.26; N, 19.34%. IR: $\tilde{v}_{max}$ (most intense peak) 1363 cm^{-1}. Electronic spectrum (MeOH): λ_{max}, nm (ε, dm^3 mol^{-1} cm^{-1}). 633 (2180), 381 (33 500), 332 (32 800). ^{1}H NMR (d_6-DMSO): δ = 6.65 (s, 2H), 8.64 (s, 2H), 9.63 (s, 1H), 11.80 (s, 1H), 13.90 (s, 1H), 15.78 (s, 1H) ppm.

Fe(PC3AH)$_2$. Anal. found: C, 58.06; H, 4.08; N, 20.71%; calculated for C$_{26}$H$_{22}$FeN$_8$O$_2$: C, 58.44; H, 4.15; N, 20.97%. IR: $\tilde{v}_{max}$ (most intense peak) 1359 cm^{-1}. Electronic spectrum (MeOH): λ_{max}, nm (ε, dm^3 mol^{-1} cm^{-1}) 637 (2440), 351 (27 800), 296 (27 300), 236 (40700). ^{1}H NMR (d_6-DMSO): δ = 6.07 (s, 2H), 7.72 (s, 1H), 8.20 (s, 3H), 10.88 (s, 1H), 12.11 (s, 1H), 13.52 (s, 1H) ppm.

Fe(PC4BBH)$_2$. Anal. found: C, 47.19; H, 2.47; N, 12.87%; calculated for C$_{26}$H$_{18}$Br$_2$FeN$_6$O$_2$: C, 47.16; H, 2.74; N, 12.69%. IR: $\tilde{v}_{max}$ (most intense peak) 1361 cm^{-1}. Electronic spectrum

(MeOH): λ_{max}, nm (ε, dm^3 mol^{-1} cm^{-1}) 640 (2620), 351 (34 800), 268 (28 300). ^{1}H NMR (d_6-DMSO): δ = 10.11 (s, 2H), 10.31 (s, 2H), 13.06 (s, 1H), 14.70 (s, 1H), 18.26 (s, 1H) ppm.

[Fe(PC3BBH)$_2$]·1/2H$_2$O. Anal. found: C, 46.18; H, 2.64; N, 12.53%; calculated for C$_{26}$H$_{19}$Br$_2$FeN$_6$O$_{2.5}$: C, 46.53; H, 2.85; N, 12.52%. IR: $\tilde{\nu}_{max}$ (most intense peak) 1361 cm^{-1}. Electronic spectrum (MeOH): λ_{max}, nm (ε, dm^3 mol^{-1} cm^{-1}) 641 (2410), 349 (28 000), 260 sh ($\sim$ 21 000). ^{1}H NMR (d_6-DMSO): δ = 9.04 (s, 1H), 9.79 (s, 1H), 10.28 (s, 1H), 10.42 (s, 1H), 13.33 (s, 1H), 15.03 (s, 1H), 19.18 (s, 1H) ppm.

[Fe(PC2BBH)$_2$]·1/2EtOAc. The precipitate from the reaction mixture was re-crystallised from ethyl acetate, which afforded dark green crystals suitable for X-ray work. Anal. found: C, 47.50; H, 3.05; N, 11.67%; calculated for C$_{28}$H$_{22}$Br$_2$FeN$_6$O$_3$: C, 47.62; H, 3.14; N, 11.90%. IR: $\tilde{\nu}_{max}$ (most intense peak) 1377 cm^{-1}. ^{1}H NMR (DMSO-d_6): δ = 1.16 (t, 3H), 1.99 (s, 3H), 4.03 (q, 2H), 7.58 (br, t, 3H), 8.78 (br, d, 6H), 9.48 (br, s, 2H), 11.25 (br, s, 2H), 12.15 (br, s, 3H) and 14.71 (br, s, 2H) ppm. Electronic spectrum (MeOH): λ_{max}, nm (ε, dm^3 mol^{-1} cm^{-1}) 624 (1580), 337 (19 300), 294 (26 000). ^{1}H NMR (d_6-DMSO): δ = 8.21 (s), 9.55 (s), 10.35 (s), 12.18 (s), 13.33 (s), 16.37 (s) ppm.

[Fe(PC4HH)$_2$]·1/2H$_2$O. Anal. found: C, 57.27; H, 3.95; N, 15.11%; calculated for C$_{26}$H$_{21}$FeN$_6$O$_{4.5}$: C, 57.26; H, 3.88; N, 15.41%. IR: $\tilde{\nu}_{max}$ (most intense peak) 1368 cm^{-1}. Electronic spectrum (MeOH): λ_{max}, nm (ε, dm^3 mol^{-1} cm^{-1}) 634 (2230), 363 (31 600), 307 (28 300), 241 (20300). ^{1}H NMR (d_6-DMSO): δ = 9.66 (s, 2H), 10.55 (s, 2H), 11.66 (s, 1H), 12.73 (s, 1H), 14.64 (s, 1H), 16.99 (s, 1H) ppm.

[Fe(PC3HH)$_2$]·1/2H$_2$O. Anal. found: C, 57.02; H, 3.61; N, 15.24%; calculated for C$_{26}$H$_{21}$FeN$_6$O$_{4.5}$: C, 57.26; H, 3.88; N, 15.41%. IR: $\tilde{\nu}_{max}$ (most intense peak) 1369 cm^{-1}. Electronic spectrum (MeOH): λ_{max}, nm (ε, dm^3 mol^{-1} cm^{-1}) 637 (3160), 353 (33 300), 260 (24 400). ^{1}H NMR (d_6-DMSO): δ = 8.55 (s, 1H), 9.68 and 9.78 (d, 3H in total), 10.96 (s, 1H), 12.11 (s, 1H), 13.59 (s, 1H), 15.80 (s, 1H) ppm.

[Fe(PCTH)$_2$]·1/2H$_2$O. Anal. found: C, 49.87; H, 3.17; N, 15.85%; calculated for C$_{22}$H$_{17}$FeN$_6$O$_{2.5}$S$_2$: C, 50.30; H, 3.26; N, 16.00%. IR: $\tilde{\nu}_{max}$ (most intense peak) 1371 cm^{-1}. Electronic spectrum (MeOH): λ_{max}, nm (ε, dm^3 mol^{-1} cm^{-1}) 635 (2090), 360 (35 500), 316 (22 800), 268 (21200). ^{1}H NMR (d_6-DMSO): δ = 10.20 (s, 1H), 10.64 (s, 1H), 11.39 (s, 1H), 16.02 (s, 1H), 18.05 (s, 1H), 24.72 (s, 1H) ppm.

[Fe(PCFH)$_2$]·H$_2$O. Anal. found: C, 53.04; H, 3.21; N, 16.96%; calculated for C$_{22}$H$_{18}$FeN$_6$O$_5$: C, 52.61; H, 3.61; N, 16.73%. IR: $\tilde{\nu}_{max}$ (most intense peak) 1386 cm^{-1}. Electronic spectrum (MeOH): λ_{max}, nm (ε, dm^3 mol^{-1} cm^{-1}) 632 (1950), 357 (32 500), 327 (24 100), 311 (23 800), 243 (16 400). ^{1}H NMR (d_6-DMSO): δ = 9.07 (s, 1H), 9.25 (s, 1H), 10.30 (s, 1H), 14.08 (s, 1H), 15.51 (s, 1H), 20.29 (s, 1H) ppm.

Physical methods

Instrumentation

Solution UV/visible spectra were measured on a Perkin-Elmer Lambda 40 spectrophotometer. Infrared spectra were measured on a Perkin-Elmer Model 1600 FT-IR spectrophotometer with compounds being dispersed as KBr discs. ^{1}H NMR and ^{13}C NMR spectra were obtained with Bruker AC200F (200 MHz) and AV400 (400 MHz) instruments with TMS as internal standard for free ligand spectra or as an external standard contained within a capillary for ^{1}H NMR spectra of all Fe^{II} complexes.

Cyclic voltammetry was performed with a BAS100B/W potentiostat employing a glassy carbon or platinum working electrode and a platinum auxiliary electrode. For non-aqueous electrochemical experiments in MeCN, a Ag/AgNO$_3$ (0.01 M in MeCN) reference electrode was used. Potentials for non-aqueous electrochemistry are cited *versus* the ferrocene/ferrocenium (Fc$^{+/0}$) couple. For voltammetry in 1 : 1 DMF : H$_2$O solution or in water, an aqueous Ag/AgCl reference electrode was employed (E° = 196 mV *vs.* NHE). Concentrations of complexes were 1–5 mM and 0.1 M Et$_4$NClO$_4$ was the supporting electrolyte for non-aqueous solvent systems or 0.1 M NaClO$_4$ for aqueous media.

Potentiometric titrations

Potentiometric titrations were performed with a Metrohm Titroprocessor under a nitrogen atmosphere in a water-jacketed chamber at 298 K as described.[19] The titrant was 0.1 M Et$_4$NOH, standardised with HCl. Data were refined by a non-linear least-squares refinement method using the program *SuperQuad*.[21]

Crystallography

Cell constants at 293 K were determined by a least-squares fit to the setting parameters of 25 independent reflections measured on an Enraf-Nonius CAD4 four-circle diffractometer employing graphite-monochromated Mo-Kα radiation (0.71073 Å) and operating in the ω-2θ scan mode within the range $2 < 2\theta < 50$ Å. The data set collected at 150 K employed an Oxford Cryosystems Cryostream Cooler (600 Series). Data reduction and empirical absorption corrections (ψ-scans) were performed with the WINGX suite of programs.[22] Structures were solved by direct methods with *SHELXS* and refined by full-matrix least-squares analysis with *SHELXL-97*.[23] All non-H atoms were refined with anisotropic thermal parameters, except C3B and C6B in the structure of [Fe(PC2BBH)$_2$]·1/2EtOAc where the data could only support partial anisotropic refinement due to the large number of parameters (two formula units in the asymmetric unit). Aryl and amino H-atoms were included at estimated positions using a riding model. Water and amide H-atoms (if any) were first located from difference maps then constrained at these positions in a similar manner to that employed for the remaining H-atoms. Molecular structure diagrams were produced with *ORTEP3*.[24] Crystal data are summarised in Table 1.

Biological methods

Materials

Chelators were dissolved in DMSO as 10 mmol dm^{-3} stock solutions and diluted in medium containing 10% foetal calf serum (Commonwealth Serum Laboratories, Melbourne, Australia) so that the final [DMSO] < 0.5% (v/v).[25] Human SK-N-MC neuroepithelioma cells were from the American Type Culture Collection (Rockville, Maryland, USA) and cultured by standard procedures.[26] This latter cell type was used as the effects of chelators on its Fe metabolism are well characterised.[16,25,27]

Table 1 Crystallographic data

	HPCNH·2H$_2$O	HPCPH	HPC2BBH·2H$_2$O	HPC3HH	[H$_2$PC3BBH]·ClO$_4$·2H$_2$O	[H$_2$PC4BBH]·ClO$_4$·H$_2$O	[Fe^{II}(PC2BBH)$_2$]·1/2CH$_3$COOC$_2$H$_5$
Formula	C$_{12}$H$_{14}$N$_4$O$_3$	C$_{12}$H$_{10}$N$_4$O	C$_{13}$H$_{14}$BrN$_3$O$_3$	C$_{13}$H$_{11}$N$_3$O$_2$	C$_{13}$H$_{15}$BrClN$_3$O$_7$	C$_{13}$H$_{13}$BrClN$_3$O$_6$	C$_{28}$H$_{22}$Br$_2$FeN$_6$O$_3$
Molecular wt	262.27	226.24	340.18	241.25	440.64	422.62	706.14
Crystal system	Triclinic	Monoclinic	Trigonal	Monoclinic	Monoclinic	Orthorhombic	Triclinic
a/Å	6.420(1)	8.469(1)	26.311(3)	4.618(1)	6.839(5)	10.434(1)	13.833(3)
b/Å	8.001(1)	13.836(2)		22.759(3)	16.527(5)	10.7200(6)	14.191(3)
c/Å	12.943(2)	9.806(2)	11.270(1)	10.663(3)	15.507(5)	14.691(2)	16.863(2)
a/°	87.76(2)						69.80(1)
β/°	76.47(2)	105.64(1)		96.98(2)	90.079(5)		89.23(1)
γ/°	80.73(1)						64.05(2)
V/Å^3	637.9(2)	1106.5(3)	6757(1)	1112.4(4)	1752.7(15)	1643.2(3)	2756.0(9)
T/K	293	293	293	293	293	293	150
Z	2	4	18	4	4	4	4
Space group	P$\bar{1}$	P2$_1$/n	R$\bar{3}$	P2$_1$/c	P2$_1$/c	Pc2$_1$n^a	P$\bar{1}$
μ/mm^{-1}	0.101	0.092	2.748	0.101	2.538	2.699	3.489
Indep. refs (R$_{int}$)	2247 (0.0117)	1941 (0.0262)	2639 (0.0801)	1964 (0.0559)	3082 (0.0264)	1699 (0.0366)	9682 (0.0906)
R$_1$ (obs. data)	0.0341	0.0400	0.0477	0.0494	0.0405	0.0386	0.0811
wR$_2$ (all data)	0.1017	0.1236	0.1179	0.1589	0.1157	0.0833	0.2568

^{a} Variant of Pna2$_1$.

^{59}Fe$_2$–transferrin labelling

Radioactive ^{59}Fe (as ferric chloride in 0.1 M HCl) was purchased from Dupont (NEN Products, Boston, Massachusetts, USA). Human apotransferrin (Sigma) was prepared and labelled with ^{59}Fe to produce ^{59}Fe-transferrin (^{59}Fe-Tf) using established methods.[26]

Iron efflux and uptake experiments

The effect of the HPCIH chelators on the release of ^{59}Fe from SK-N-MC cells pre-labelled with ^{59}Fe-Tf and their ability to prevent ^{59}Fe uptake from ^{59}Fe-Tf were determined using standard procedures.[25,27,28] Briefly, efflux of ^{59}Fe from cells was examined after a 3 h preincubation of cells at 37 °C with ^{59}Fe-Tf ([Tf] = 0.75 μmol dm^{-3}; [Fe] = 1.5 μmol dm^{-3}). The cells were then washed four times with ice-cold phosphate buffered saline (PBS) followed by a 3 h reincubation at 37 °C in the presence of medium alone (control) or each of the chelators at 25 μmol dm^{-3}. The overlying medium was then removed and placed in γ-counting tubes. The cells were removed from the culture dish in 1 cm^3 of PBS using a plastic spatula and added to separate γ-counting tubes.

Internalised ^{59}Fe uptake from ^{59}Fe-Tf by SK-N-MC neuroepithelioma cells was examined in the presence of the chelators. Cells were incubated for 3 h at 37 °C with ^{59}Fe-Tf ([Tf] = 0.75 μmol dm^{-3}; [Fe] = 1.5 μmol dm^{-3}) in the presence and absence of chelators (25 μmol dm^{-3}). The cells were then washed four times with ice-cold PBS and incubated with ice-cold PBS containing the general protease, Pronase (1 g dm^{-3}), for 30 min at 4 °C to separate internalised and membrane-bound ^{59}Fe.[26] Cells were removed from the substratum using a plastic spatula in the Pronase solution and centrifuged at 14000 × g for 1 min. The supernatant (membrane-bound ^{59}Fe) and pellet (internalised ^{59}Fe) were then separated using a Pasteur pipette and transferred to γ-counting tubes for the determination of radioactive ^{59}Fe.

DNA plasmid degradation

The ability of the chelators to protect (or potentiate) DNA plasmid degradation in the presence of Fe^{II} and H$_2$O$_2$ was examined

using published techniques.[17] The chelators were incubated for 30 min in the presence of Fe^{II} (10 μmol dm^{-3}), hydrogen peroxide (1 mmol dm^{-3}) and plasmid DNA (10 μg cm^{-3}) in the presence and absence of chelators. Samples were then loaded onto a 1% agarose gel and electrophoresed for 1 h at 90 V.[17]

Results and discussion

The HPCIH analogues: structure and properties

We previously published the crystal structures of the free ligands HPCIH, HPCBH, HPCFH[29] and HPCAH.[19] Here we report the additional crystal structures of HPCNH·2H$_2$O, HPCPH, HPC2BBH·2H$_2$O and HPC3HH (Fig. 3).

The bond lengths and angles are as expected for compounds of this type.[29] In every case, the pyridyl N-atom was *anti* with respect to the imine N-atom, which avoids repulsion between the H-atoms attached to C4 and C6. As a consequence, the molecule is unfavourably disposed to coordinate a metal ion through the pyridyl N-atom (N1), imine N-atom (N2) and carbonyl O-atom (O1). Most of the ligands, including HPCIH,[29] are effectively planar with N1–C5–C6–N2, C6–N2–N3–C7 and N3–C7–C8–C9 torsion angles close to 180°. However, the 2-bromophenyl ring in HPC2BBH is twisted about the C7–C8 bond, which may be attributed to the steric effect of the *ortho* Br atom, forcing the ring to rotate by a much greater extent than the other analogues.

The salts (H$_2$PC3BBH)ClO$_4$·2H$_2$O and (H$_2$PC4BBH)ClO$_4$·H$_2$O (Fig. 4) were crystallised from dilute perchloric acid solutions (pH 2). The pyridyl N-atom (N1) is identified as the site of protonation. Bond lengths and angles are not affected by the protonation as expected, which remain comparable to the rest of the ligands in the series. In contrast to HPC2BBH (Fig. 3), the bromine atoms in (H$_2$PC3BBH)$^+$ and (H$_2$PC4BBH)$^+$ (Fig. 4) no longer impose any steric influence on the conformation of the phenyl ring and thus the molecules are virtually planar (N1–C5–C6–N2 and N3–C7–C8–C9 torsion angles at 180° and 174.2° for (H$_2$PC3BBH)$^+$ and 175.1° and 168.4° for (H$_2$PC4BBH)$^+$, respectively).
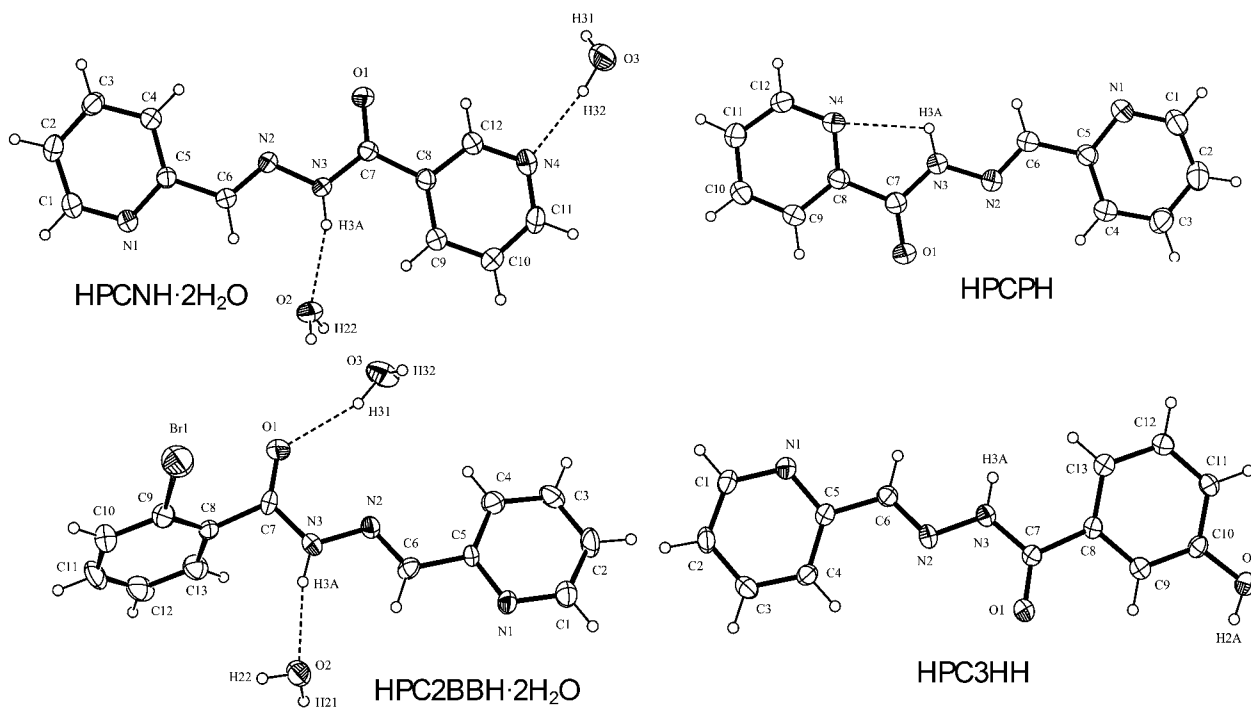
Fig. 3 ORTEP drawings of the neutral hydrazones: HPCNH·2H$_2$O, HPCPH, HPC2BBH·2H$_2$O and HPC3HH (30% probability ellipsoids).
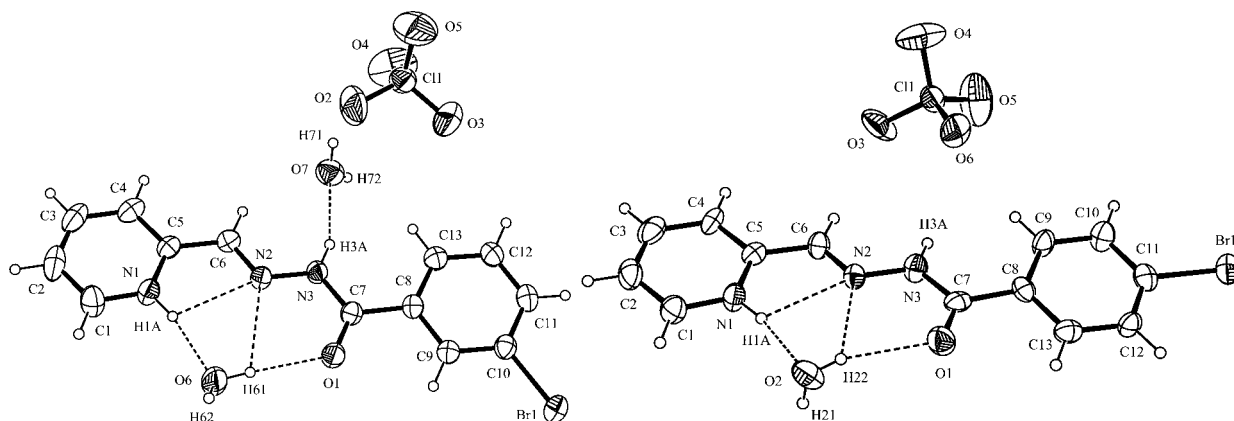

Fig. 4 View of [H$_2$PC3BBH]ClO$_4$·2H$_2$O (left) and [H$_2$PC4BBH]ClO$_4$·H$_2$O (right) (30% probability ellipsoids).

In contrast with the structures of the neutral hydrazones in Fig. 3, the conformations of the protonated hydrazones are quite different. The pyridyl and imine N-atoms are now *syn* and the ligands are primed for tridentate coordination (Fig. 4). Interestingly, a water molecule occupies the position normally taken by a coordinated metal ion, H-bonds replacing coordinate bonds in this instance. The water protons donate H-bonds to the imine-N and carbonyl-O atoms, while the water O-atom accepts an H-bond from the pyridinium NH group (Fig. 4).

Protonation constants

Charged chelators (at physiological pH 7.4) are hindered in their passage across cellular membranes and cannot gain access to intracellular Fe pools nor can they be absorbed from the gut.[1,30] The protonation constants of the HPCIH series of ligands were determined and the results appear in Table 2. The assignment of

pK$_a$ values of ionisable protons in the HPCIH analogues conforms to reports of similar aroylhydrazones.[30–36] The first protonation constant (pK$_1$) is associated with the hydrazone N–N*H*–C=O group, while the lower pK$_a$ value (pK$_2$) is assigned to protonation of the 2-pyridyl ring, which is supported by crystallographic evidence reported here (Fig. 4).

A significant inductive effect by the non-coordinating aromatic substituent on pK$_1$ is apparent. The electron-withdrawing isonicotinoyl group accounts for the low pK$_1$ value (9.17(1) for HPCIH). Conversely, the electron-donating 4-aminobenzoyl group accounts for the highest pK$_1$ value (11.63(3) for HPCAH). The value of pK$_1$ is important in determining the amount of ionised ligand at physiological pH (7.4) and also has a bearing on the proton-independent formation constants[19] (see below). In summary, most of the HPCIH analogues will be dominantly neutral at pH 7.4. Indeed, HPCTH as one of our lead compounds has been shown to penetrate cells and induce

Table 2 Protonation constants and partition coefficients of the HPCIH analogues

	pK_1 (amide-N)	pK_2 (2-pyridyl-N)	log P (octanol–H_2O)
HPCIH	9.17(1)	3.61(1)	1.98
HPCNH	9.34(3)	3.50(2)	1.94
HPCPH	9.56(4)	3.84(4)	2.32
HPCBH	9.78(1)	3.37(1)	2.84
HPCAH	11.63(3)	3.83(4)	2.31
HPC3AH	10.61(2)	3.49(1)	1.94
HPC4BBH	9.61(3)	3.80(4)	4.17
HPC3BBH	10.12(2)	3.28(2)	3.70
HPC2BBH	9.96(5)	3.32(3)	3.06
HPC4HH	9.38(4)	3.26(4)	2.78
HPC3HH	9.25(1)	3.21(1)	2.94
HPCTH	9.38(3)	4.15(2)	2.79
HPCFH	10.25(2)	3.18(1)	2.47

the release of intracellular Fe[16] and is an orally-active Fe chelator in mice.[18]

Fe complexes

The syntheses of Fe[II] complexes of the HPCIH analogues in pure form required carefully controlled conditions or else mixtures of mono- and bis-ligand complexes were obtained. Ferrous perchlorate was used as the salt, a large excess of triethylamine (20 equivalents) was added and the solvent was MeCN. This procedure was a successful general method to synthesise all FeL$_2$ complexes from the HPCIH analogues. A notable exception was HPCPH, where a partially oxidised di-Fe[II], triple helical Fe$_2$(L$_2$L') mixed ligand (hydrazone/hydrazine) complex was formed.[37] The peculiarities of this compound arise from participation of the 2-pyridyl N-donor adjacent to the carbonyl group.[37] No Fe complexes of this ligand are reported here.

Upon complexation of the HPCIH ligands, the IR vibrations involving the –HN–C=O– ('amide') functional group of the hydrazone ligands were most affected.[38,39] The NH proton is lost upon complexation and the amide group is converted to an enolate form *i.e.* –N–C=O–Fe. The carbonyl stretching frequency seen in the free ligands (1630–1700 cm^{-1}) shifts to lower frequency. Given the complexity of the IR spectra in the range 1200–1600 cm^{-1}, an unambiguous assignment is difficult due to overlapping C=C and C=N vibrations from the aromatic rings. However, all Fe complexes exhibit a strong IR absorption at *ca.* 1380 cm^{-1} which was not observed in the free ligands and is probably due to the –N=C–O–Fe moiety.

The electronic spectra of the Fe[II] complexes of the HPCIH series in methanol were similar and each featured an intense, broad, asymmetric maximum at *ca.* 640 nm. By analogy with the closely related low spin Fe[II] complexes of the HPKIH analogues (Fig. 2),[36] this transition is most likely of metal-to-ligand charge-transfer (MLCT) origin. All complexes exhibit intense ligand-based transitions in the near UV region at *ca.* 350 nm and 280 nm. A bathochromic shift is observed in these ligand-based transition bands as the aromatic substituent on the ligand becomes more strongly electron-donating. HPCAH, which bears the most strongly electron-donating substituents of the series, has the lowest energy maxima at 381 nm and 332 nm.

The ^{1}H NMR spectra of the Fe[II] complexes measured in d_6-DMSO exhibited broad and downfield-shifted singlets for all

protons (regardless of their environment) in contrast to the well resolved multiplets seen in the spectra of the free ligands. This feature is due to paramagnetism arising from a high-spin/low-spin equilibrium in solution. No time dependence in the spectra was noted, so paramagnetic impurities from aerial oxidation of the complex can be ruled out. The number of peaks seen in each ^{1}H NMR spectrum was always less than the number of chemically distinct protons. The magnitude of the paramagnetic shift is indicative of the amount of high spin Fe[II] present and this varied considerably across the series. A full and accurate assignment of each NMR spectrum, as performed for the analogous Fe(PKIH)$_2$ series,[36] was not feasible but there are some clear trends apparent across the series of twelve Fe complexes. The non-coordinating aromatic/heterocyclic ring protons appear least affected by paramagnetism and are seen in the range of 7–10 ppm. The remaining peaks are considerably broader and appear well downfield (> 10 ppm). These correspond to the 4 pyridyl protons and the single azomethine proton. However, in no case were all 5 peaks seen. The complexes Fe(PCNH)$_2$, Fe(PC4AH)$_2$ and Fe(PC3AH)$_2$ each exhibited 4 of the 5 expected peaks from the pyridine carbaldehyde moiety while all other complexes gave only 3 resonances with a large downfield shift. In our previous study with the Fe(PKIH)$_2$ analogues,[36] we showed that the proton most affected by paramagnetism was that in the 6-position of the coordinated pyridyl ring although in that case the paramagnetism was only very mild by comparison. Extrapolating to this system, we believe that the NMR resonance for the proton attached to atom C1 in Fig. 2 and 3 of all complexes was never seen in our NMR spectra due to an extremely large paramagnetic shift (and broadening). Thus the most downfield shifted proton of the four seen in the spectra of Fe(PCNH)$_2$, Fe(PC4AH)$_2$ and Fe(PC3AH)$_2$ (the least paramagnetic compounds of this series) is presumably from the azomethine proton, which like the proton adjacent to the coordinated pyridyl N-atom is in closest proximity to the Fe ion and subject to the greatest influence of its paramagnetism.

The complex [Fe(PC2BBH)$_2$]·1/2EtOAc was successfully crystallised from ethyl acetate and its crystal structure determined at low temperature (150 K). The asymmetric unit comprises two complex molecules and a single ethyl acetate solvent molecule. Fig. 5 shows one complex molecule from the asymmetric unit. This bis-ligand complex is representative of the preferred binding mode of the HPCIH analogues and is the first bis-ligand Fe complex structurally characterised from this series. The coordination about Fe[II] can be described as distorted octahedral, with the two tridentate ligands arranged in a meridional fashion, orthogonal to each other. The bite angles defined by the two consecutive five-membered chelate rings of the coordinated hydrazone are *ca.* 80°, thus resulting in the distorted octahedral coordination geometry. The bond lengths are characteristic of low spin Fe[II] and very similar to those reported for the related Fe[II] complexes of the HPKIH analogues.[36]

In the Fe(PC2BBH)$_2$ complex, the 2-bromophenyl rings are twisted away from the plane of the ligands by *ca.* 45° (Fig. 5), similar to that seen in the structure of the free ligand (Fig. 3). The two complexes within the asymmetric unit exhibit slightly different conformations. In the molecule shown in Fig. 5, one bromine atom (Br1B) is *syn* with respect to the carbonyl group, while the other (Br1A) is *anti*, whereas in molecule 2 (not shown) both bromine atoms are *syn* with respect to their adjacent carbonyl groups.
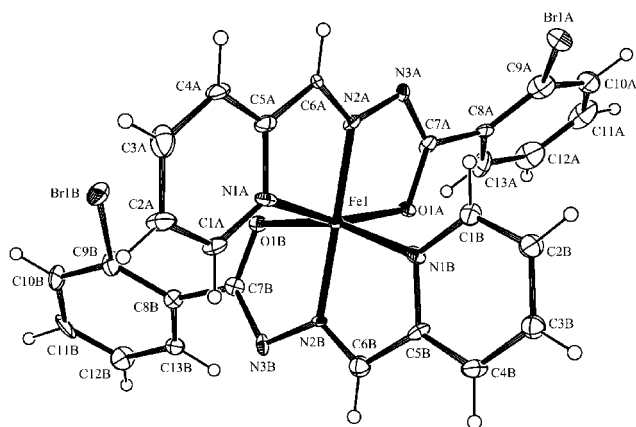
Fig. 5 ORTEP drawing of one of the two independent Fe(PC2BBH)$_2$ molecules (30% probability ellipsoids): selected bond lengths (Å) Fe1–N1A 1.95(1), Fe1–N1B 1.94(1), Fe1–N2A 1.86(1), Fe1–N2B 1.866(9), Fe1–O1A 1.987(8), Fe1–O1B, 1.979(8), C7A–N3A 1.32(2), C7B–N3B 1.35(2), C7A–O1A 1.30(1), C7B–O1B 1.29(1).

Complex formation constants

The Fe^{II} complex formation constants of the HPCIH series (in water) have been determined and are given in Table 3. Equilibrium constants for the formation of both mono- ([FeL]$^+$) and bis-ligand (FeL$_2$) complexes were calculated. Under the conditions of the experiment, charge-neutral bis-ligand complexes of the typical formula Fe(PCIH)$_2$ are the prevailing species at physiological pH of 7.4, while mono-ligand complexes [Fe(PCIH]$^+$ begin to form at pH ≈ 3. This is significant, as it means that a bis-ligand Fe^{II} complex formed within the cell may freely permeate the cell membrane to re-enter the plasma for excretion, since it carries no charge.[40] Hence, the neutral charge of the ligand and Fe complex may explain, at least in part, the high Fe chelation efficacy of many of these ligands, including HPCTH which has been examined *in vitro* and *in vivo*.[16,18]

The pM scale (–log$_{10}$[uncomplexed metal ion] at pH 7.4 after equilibration of 1 μmol dm^{-3} metal ion and 10 μmol dm^{-3} ligand)[41,42] allows comparison of the relative ability of different

ligands to bind a metal under comparable physiological conditions. In simple terms, the pM value is calculated from the proton-dependent stability constant, which is in turn derived from the ligand protonation constants and complex formation constants. The pM values for the formation of Fe^{III} complexes of transferrin,[41,42] as well as Fe^{II} and Fe^{III} complexes of DFO[41–43] and H$_2$PIH[44] are tabulated for comparison (Table 3). The variation in pM values for the formation of Fe^{II} complexes is relatively small across the HPCIH series. In fact, the small difference in affinity for Fe^{II} among the HPCIH analogues is inadequate to account for the difference in their biological activity (see below). This clearly indicates that factors other than metal selectivity and affinity are responsible for the diversity in Fe chelation efficacy within the series and justify the assessment of factors such as lipophilicity, as described below.

The HPCIH analogues possess higher affinity for Fe^{II} than does DFO (pM = 6.13). On the other hand, the high affinity of the hexadentate DFO for Fe^{III} is rational, since it is a bacterial siderophore "designed" to sequester Fe^{III} specifically, coordinating through six hard O-donors.[45,46] In contrast, the HPCIH analogues coordinate through the pyridyl-N, imine-N and carbonyl-O atoms, furnishing a softer N$_4$O$_2$ coordination sphere which leads to a preference for divalent over trivalent iron. Of note, the monobasic HPCIH analogues form charge-neutral bis-ligand complexes with divalent metal ions[19] (including Fe here).

Electrochemistry

In pure MeCN solution the Fe(PCIH)$_2$ analogue complexes displayed two reversible redox responses. The redox potentials are shown in Table 4 and a typical cyclic voltammogram of Fe(PCFH)$_2$ in MeCN, is illustrated in Fig. 6. The higher potential voltammetric responses ($E^{o'}$ between −200 mV and 0 mV *vs.* Fc$^{+/0}$ (MeCN)) are assigned to the Fe$^{III/II}$ redox couple. The lower potential responses (Table 4) fall within a rather narrow range and their current magnitude is consistent with a net two electron process by comparison with the obligate single electron high potential (Fe$^{III/II}$) couple. The only redox active moiety common to the entire series (apart from the metal itself) is the coordinated

Table 3 Partition coefficients for Fe complexes of the HPCIH analogues, their proton-independent Fe complex formation constants and pM values. Data for transferrin, DFO and H$_2$PIH included for comparison

	log P (octanol–H$_2$O)	log β_1	log β_2	pM (Fe^{II})	pM (Fe^{III})
Fe(PCIH)$_2$	1.89	7.02(2)	13.37(2)	6.50	—
Fe(PCNH)$_2$	1.85	7.12(4)	14.38(3)	6.67	—
Fe(PCBH)$_2$	2.89	7.07(2)	13.81(2)	6.20	—
Fe(PC4AH)$_2$	1.99	8.47(3)	17.58(3)	6.11	—
Fe(PC3AH)$_2$	2.25	7.54(2)	14.92(2)	6.09	—
Fe(PC4BBH)$_2$	2.67	7.00(8)	14.58(6)	6.43	—
Fe(PC3BBH)$_2$	3.52	7.14(8)	14.93(3)	6.44	—
Fe(PC2BBH)$_2$	3.01	6.93(5)	13.60(4)	6.10	—
Fe(PC4HH)$_2$	2.67	6.37(3)	11.81(5)	6.10	—
Fe(PC3HH)$_2$	2.60	6.43(1)	12.35(1)	6.15	—
Fe(PCTH)$_2$	3.00	7.30(2)	14.18(4)	6.62	—
Fe(PCFH)$_2$	2.20	7.56(2)	14.64(2)	6.20	—
Fe$_2$-transferrin	—	—	—	—	25.6[a]
Fe(DFO)				6.13[b]	26.6[b]
Fe(HPIH)(PIH)	3.1[c]			7.14[d]	27.7[d]

[a] Ref. 41 and 42. [b] Recalculated from published proton independent stability constants (ref. 43). [c] Ref. 49. [d] Recalculated from published proton independent stability constants (ref. 44).

Table 4 Redox potentials of the Fe^{II} complexes of HPCIH series in 100% MeCN and 50% DMF : H$_2$O. All couples in MeCN were totally reversible, while in DMF : H$_2$O only the anodic (Fe^{II} to Fe^{III}) peak potential (E_{pa}) is listed due to total irreversibility of the response

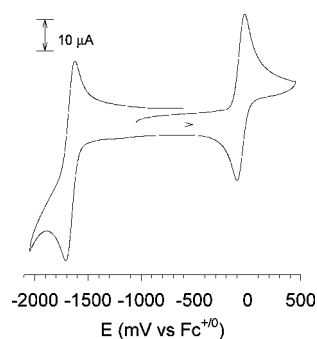|	MeCN ($E^{o'}$ vs. Fc$^{+/0}$)/mV		50% DMF : H$_2$O (E_{pa} vs. NHE)/mV
	[FeL$_2$]$^{+/0}$	[FeL$_2$]$^{0/-}$	[FeL$_2$]$^{+/0}$
Fe^{II}(PCIH)$_2$	−11	−1585	616
Fe^{II}(PCNH)$_2$	−53	−1647	593
Fe^{II}(PCBH)$_2$	−105	−1697	531
Fe^{II}(PC4AH)$_2$	−206	−1766	426
Fe^{II}(PC3AH)$_2$	−133	−1711	520
Fe^{II}(PC4BBH)$_2$	−80	−1677	543
Fe^{II}(PC3BBH)$_2$	−66	−1633	544
Fe^{II}(PC2BBH)$_2$	−67	−1674	542
Fe^{II}(PC4HH)$_2$	−88	−1717	497
Fe^{II}(PC3HH)$_2$	−107	not obs.	534
Fe^{II}(PCTH)$_2$	−65	−1664	544
Fe^{II}(PCFH)$_2$	−63	−1665	583

Fig. 6 Cyclic voltammogram of Fe(PCFH)$_2$ in MeCN. Direction of initial sweep shown by arrow and the sweep rate was 100 mV s^{-1}.

2-pyridyl ring. The two electron stoichiometry is indicative of overlapping single electron reductions of the coordinated pyridyl ligands *i.e.* there is no interaction between the two ligands and their redox potentials are too close to be resolved. This is similar behaviour to that reported in the electrochemistry of the related Fe(PKIH)$_2$ complexes.[36] Of note, is the significantly more negative potentials exhibited by Fe(PCAH)$_2$. This is consistent with the strong electron-donating effect of the 4-aminophenyl substituent disfavouring both metal and ligand based reductions. At the other end of the series, Fe(PCIH)$_2$ displayed the most positive potentials, in this case most likely due to the strongly electron-withdrawing isonicotinoyl ring. A similar trend has been reported in the related Fe(PKIH)$_2$ series.[36]

Electrochemistry of Fe(PCIH)$_2$ in a 1 : 1 mixture of DMF/water was investigated to provide more physiologically relevant redox potentials. Due to the limited aqueous solubility of the complexes, a minimum of 50% DMF was required to keep all complexes in solution and enable comparisons across the entire series. Due to the narrower potential window offered by this solvent, only the Fe$^{III/II}$ couple was investigated.

Fig. 7 illustrates the cyclic voltammogram of Fe(PCIH)$_2$ in 1 : 1 DMF/water mixture at pH 7. All of the Fe(PCIH)$_2$ analogues displayed totally irreversible redox responses around 500 mV (*vs.* NHE) at pH = 7 (Table 4) that are consistent with a chemical reaction following oxidation (EC mechanism). Previously, we discussed this mechanism in the related Fe(PKIH)$_2$ analogues
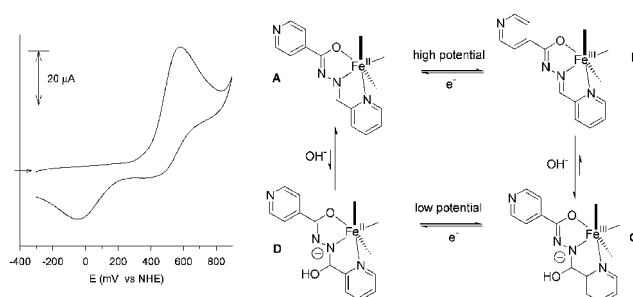

Fig. 7 (left) Cyclic voltammogram of Fe(PCIH)$_2$ in 50% aqueous DMF at pH 7 (sweep rate 100 mV s^{-1}) and (right) proposed 'square' electrochemical scheme (only one coordinated ligand is shown for clarity but both are assumed to undergo the same reaction simultaneously).

and modelled the electrochemistry using digital simulation.[36,37] The proposed mechanism adapted to this system is also shown in Fig. 7 (right). Briefly, in MeCN, only the reversible single electron exchange between compounds **A** and **B** (top line) was relevant. However, in the presence of water, the ferric complex undergoes rapid nucleophilic attack by hydroxide to produce compound **C**. The latter is reduced at a much lower potential (*ca.* 0 mV) to give compound **D**. Compound **D** is also unstable and eliminates water to restore the original Fe^{II} complex **A** in a process that may be cycled indefinitely.

The electrochemistry of the other Fe(PCIH)$_2$ analogues in the same solvent was similar and in all cases a totally irreversible Fe$^{III/II}$ couple was identified. The redox potentials followed the same trend seen in the non-aqueous electrochemistry, indicating that the inductive effects of the non-coordinating aromatic rings are qualitatively similar in both water and MeCN. Due to the irreversibility of the Fe$^{III/II}$ couple in DMF : water, only the anodic peak potential is shown in Table 4. It is notable that the peak position was sweep rate independent, thus the initial redox reaction is associated with a rapid heterogeneous electron transfer.

These results are very interesting when compared with those of the structurally similar Fe(PKIH)$_2$ analogues, where the ferric complexes underwent hydrolysis at a much slower rate (pseudo first order rate constants 2–50 s^{-1})[36] than the Fe(PCIH)$_2$ analogues observed here. At sweep rates of 1 V s^{-1} an appreciable cathodic ([Fe^{III}(PKIH)$_2$]$^{+}$ to Fe^{II}(PKIH)$_2$) wave was seen. Even at sweep rates as high as 20 V s^{-1} no cathodic (Fe^{III} to Fe^{II}) response in the vicinity of the initial anodic peak around 500 mV could be seen for the Fe(PCIH)$_2$ complexes. Thus, there was an order of magnitude increase in the rate of attack on the ferric complexes of the HPCIH analogues. The Fe$^{III/II}$ redox potentials of the Fe(PKIH)$_2$ complexes[36] are essentially the same as the corresponding couples for the Fe(PCIH)$_2$ analogues reported here. The only structural difference is the replacement of the non-coordinating 2-pyridyl group in the HPKIH analogues with an H-atom in the HPCIH series. Indeed, it is the C-atom to which these groups are attached that we propose is the target for nucleophilic attack by OH^{-} and evidently this reaction occurs much more slowly in the HPKIH analogues. One obvious explanation is that the pyridyl ring provides steric hindrance to nucleophilic attack (compared with an H-atom). However, there could be an inductive effect from the 2-pyridyl ring that lowers the electrophilicity of the attached C-atom, but in the absence of other analogues bearing different substituents at this position it is difficult to comment further.

Partition coefficients

The rate of passive diffusion of a compound across biological membrane and into cells will be a function of lipophilicity, conveniently quantified by its partition coefficient (log P) between 1-octanol and water.[47] In previous studies on analogues of H_2PIH[48,49] and deferiprone (L1) (Fig. 1),[50] and also other Fe chelators,[51] it was observed that the relationship between Fe mobilisation activity and log P of these compounds depends not only on the partition coefficients of the ligands, but also on the partition coefficients of their Fe complexes. In this study, the 1-octanol–water partition coefficients of the HPCIH analogues and their Fe^{II} complexes, respectively, were determined by published methods.[52] In the case of the Fe complex partition coefficients, all solutions were purged with nitrogen and sealed to prevent Fe^{II} oxidation. The 1-octanol–water partition coefficients of the HPCIH analogues and their Fe^{II} complexes are given in Tables 2 and 3.

All of the HPCIH analogues have log P equal to or greater than 2 (Table 2), with the two most lipophilic ligands of the series, HPC3BBH and HPC4BBH, displaying log P values of 3.70 and 4.17, respectively. The Fe^{II} complexes of the HPCIH analogues possess similar partition coefficients to their free ligands (Table 3). The majority of the biologically active compounds examined by Hansch *et al.* have maximum activity at values of log P between 2 and 6.[47,53] Compounds with high log P values are sparingly soluble in aqueous media (and problematic in terms of drug delivery) and thus a balance between hydrophobicity and aqueous solubility needs to be found. Edward *et al.* reported that the H_2PIH analogues have maximum activity in releasing ^{59}Fe from reticulocytes when they have intermediate values of log P [free ligand] ≈ 2.8 and log P [Fe^{III} complex] ≈ 3.1.[49,54] Most of the HPCIH analogues have log P [free ligand] and log P [Fe^{II} complex] values within this 'optimal' range.

Cellular Fe efflux and uptake experiments

The ability of the HPCIH analogues to gain access to intracellular Fe is central to their potential use in the treatment of Fe overload. To examine the efficacy of a chelator to deplete cellular Fe pools we implemented established methods, namely Fe efflux and uptake experiments using SK-N-MC cells, to investigate this.[7,25,52,55,56] The Fe efflux studies (Fig. 8A) assess the ability of a chelator to penetrate the cell membrane and bind and mobilize[59] Fe from intracellular Fe pools that have been pre-labelled by incubation with ^{59}Fe-Tf. This determines if a chelator can enter the cell and leave with cellular ^{59}Fe bound to it. We also examined the effects of the PCIH analogues at preventing cellular ^{59}Fe uptake from ^{59}Fe-Tf (Fig. 8B). This latter property also necessitates membrane permeability and examines the ability of the ligand to compete with the cell for ^{59}Fe released from ^{59}Fe-Tf in the endosome. As internal controls, we have also assessed the well characterised Fe chelators, DFO and H_2PIH (Fig. 1). All the results are compared to control samples prepared in the absence of chelator.

As is evident from Fig. 8A, DFO showed only modest ^{59}Fe efflux activity (13% cellular ^{59}Fe release) relative to the control (7% cellular ^{59}Fe release with no chelator), which was consistent with our previous work.[16,25,57] This low activity was due to the hydrophilicity and low membrane permeability of DFO.[7,57] In contrast, H_2PIH showed marked efficacy leading to the release
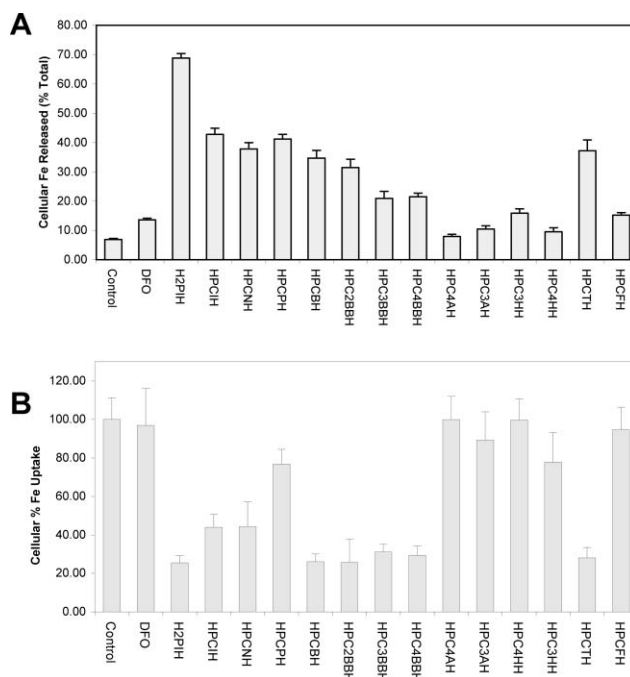

Fig. 8 The effect of DFO, H_2PIH and the HPCIH analogues at 25 μmol dm^{-3} on: (A) ^{59}Fe efflux from pre-labelled SK-N-MC neuroepithelioma cells and (B) their ability to prevent ^{59}Fe uptake from ^{59}Fe-Tf by SK-N-MC neuroepithelioma cells. Results in (A) are presented as ^{59}Fe efflux as a percentage of total cellular ^{59}Fe, while the data in (B) are expressed as a percentage relative to control with no chelator present (*i.e.* 100% uptake of ^{59}Fe). Data are presented as the mean ± SD of 5 replicates in a typical experiment of two separate experiments performed.

of 69% of cellular ^{59}Fe which is ten-fold higher than the control (Fig. 8A). In fact, H_2PIH was the most effective chelator screened in this investigation and its activity was comparable to that observed in our previous studies.[25,27]

All chelators from the HPCIH series except those with aminophenyl, hydroxyphenyl or furan substituents were significantly ($p < 0.01$) more effective than DFO in releasing ^{59}Fe from prelabelled cells (Fig. 8A). No significant effects due to isomerism in the analogues with bromophenyl, hydroxyphenyl, aminophenyl and pyridyl groups in various positions were found. The most effective analogues were HPCIH, HPCNH, HPCPH, HPCBH and HPCTH.

The ability of the HPCIH analogues to inhibit cellular ^{59}Fe uptake from ^{59}Fe-Tf is shown in Fig. 8B. Note that in this case, an effective chelator will reduce uptake of ^{59}Fe from ^{59}Fe-Tf leading to a marked decrease of intracellular ^{59}Fe relative to the control without chelator. In agreement with previous studies, DFO showed very little activity at inhibiting ^{59}Fe uptake from Tf,[7,57] while H_2PIH markedly reduced[59] Fe uptake to 25% of the control. As observed in the ^{59}Fe mobilisation study (Fig. 8A), the HPCIH analogues bearing amino, hydroxyl or furoyl substituents were largely ineffective at preventing ^{59}Fe uptake from ^{59}Fe-Tf (Fig. 8B). Chelators HPCBH, HPC2BBH, HPC3BBH, HPC4BBH and HPCTH were the most effective ligands of the HPCIH analogues. Indeed, the ligands showed efficacy comparable to H_2PIH at preventing ^{59}Fe uptake from ^{59}Fe-Tf to 26–31% of the control (Fig. 8B).

Considering these latter data showing that the best HPCIH analogues have comparable activity to H$_2$PIH at preventing ^{59}Fe uptake, it is of interest that the ability of the HPCIH analogues at inducing ^{59}Fe mobilisation from cells was much less than H$_2$PIH (Fig. 8A). Indeed, the HPCIH ligands are more effective at inhibiting ^{59}Fe uptake from ^{59}Fe-Tf than mobilising intracellular ^{59}Fe. After receptor-mediated endocytosis of diferric transferrin (Fe-Tf), Fe is released within the endosome and reduced to Fe^{II} where it is then transferred to the divalent cation transporter (DCT1).[1,4] This latter molecule transports Fe^{II} across the membrane and into the cellular labile Fe pool.[1,58] Then Fe is either used for incorporation into proteins or stored within ferritin. The fact that the HPCIH analogues are very successful in preventing ^{59}Fe-uptake, may reflect a kinetic effect whereby Fe is intercepted by the chelators *en route* before it is stored. In contrast, in cells prelabelled with ^{59}Fe-Tf, both Fe^{II} and Fe^{III} exist intracellularly[59] and the ability of the HPCIH analogues to bind predominantly Fe^{II} may disadvantage their activity relative to H$_2$PIH which binds both redox states.[44,60]

In terms of the activity of the ligands in both ^{59}Fe mobilization and ^{59}Fe uptake assays, the most effective HPCIH series chelators were HPCBH and HPCTH which showed high activity in both studies. On inspection of their physical properties (Table 2) and those of their Fe complexes (Table 3), the intermediate log P values coupled with favourable ionisation constants that lead to charge neutral chelators and Fe^{II} complexes appears to be an ideal combination for effective Fe chelation. On the other hand, it appears that hydrophilic substituents such as amino or hydroxyl, irrespective of their position on the phenyl ring, have a deleterious effect on Fe binding efficacy as found for other aroylhydrazones.[55] Hence, such groups as well as the furan substituent which also led to poor Fe chelation efficacy, should be avoided in the future design of ligands of this class.

DNA plasmid degradation

Upon complexation of intracellular Fe by a chelator, Fe may be rendered redox active and promote Fenton chemistry where Fe^{II} catalytically decomposes H$_2$O$_2$ to generate hydroxyl radicals and other ROS.[1] These ROS can cause adverse effects to normal cellular function and proliferation.[17,61] Alternatively, chelators such as DFO can bind Fe and prevent Fenton chemistry.[17]

Hence, clearly the redox activity of the Fe complex is vital to determine for assessing its use as a clinically effective agent. The plasmid single and double strand-break assay was used to determine the ability of the chelators to cause DNA strand breaks through Fenton chemistry.[17,62–65] A single strand break causes conversion of supercoiled (SC) DNA into the open circular (OC) form, while a double strand break results in the SC form being converted to linear (L) DNA.

For simplicity, comparisons between all the HPCIH analogues and controls were made based on the percentage of SC DNA remaining after the assay and these data are summarised in Fig. 9 and 10. A number of different controls were used in these studies.[17] These included, plasmid treated with the restriction enzyme *Bam*H1 which resulted in complete conversion to L DNA *i.e.* 0% SC DNA (Fig. 9, lane 2); untreated plasmid (Fig. 9, lane 3) and plasmid treated with hydrogen peroxide (Fig. 9, lane 4) that appeared on gels as primarily the SC DNA band. When plasmid
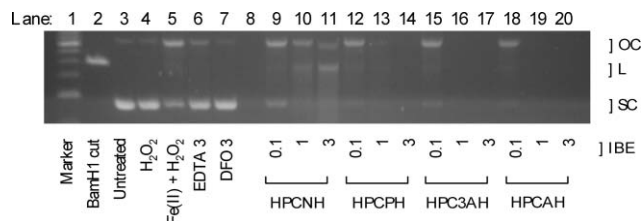

Fig. 9 Typical plasmid Fe^{II}-mediated degradation assay of EDTA, DFO and several HPCIH analogues (HPCNH, HPCPH, HPC3AH and HPCAH). The HPCIH analogues at iron-binding equivalent (IBE) ratios of 0.1, 1 and 3 were incubated for 30 min in the presence of Fe^{II} (10 µM), hydrogen peroxide (1 mM) and plasmid DNA (10 µg mL^{-1}). Samples were loaded onto a 1% agarose gel and electrophoresed for 1 h at 90 V. Results are from a typical experiment of a total of 3 performed.
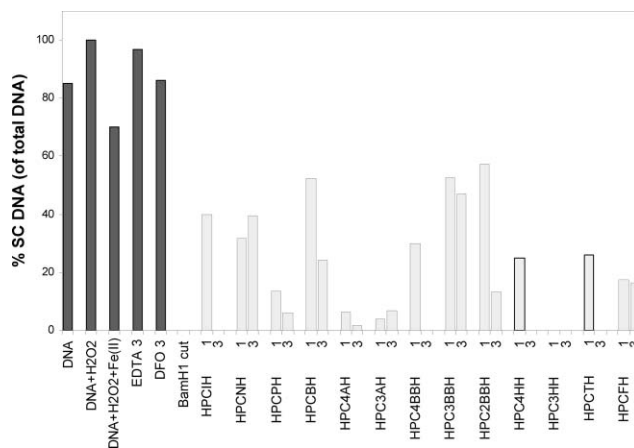

Fig. 10 Densitometric analysis of plasmid Fe^{II}-mediated degradation assay of EDTA, DFO and all the HPCIH analogues examined in this study. The experimental procedure is the same as that described in Fig. 9. Results are from a typical experiment of a total of 3 performed.

was treated with Fe^{II} and hydrogen peroxide (Fig. 9, lane 5), SC DNA was partially converted to the OC form. We also examined various Fe to chelator stoichiometries in our study. These are represented here as so-called "iron binding equivalents" (IBE).[17] An IBE of one indicates a stoichiometric ratio of Fe to ligand such that the octahedral coordination sphere of Fe is satisfied (*i.e.* 1 Fe atom to 2 tridentate HPCIH ligands, or 1 Fe atom to 1 hexadentate DFO ligand *etc*).[17] An IBE of 0.1 indicates only about 10% of Fe will be complexed, while an IBE of 3 means that there will be an excess of uncomplexed ligand and this will favour complexation in the case where the formation constants are only modest (see Table 3).

In the presence of both Fe^{II} and H$_2$O$_2$, both EDTA and DFO were protective of SC DNA at IBE of 3 (Fig. 9; lanes 6 and 7, respectively), in agreement with previous work.[17,66] However, HPCNH, HPCPH, HPC3AH and HPCIH in the presence of Fe^{II} and H$_2$O$_2$ stimulated plasmid degradation, leading to a marked decrease in SC DNA as the IBE increased to 3 (Fig. 9; lanes 9–20).

Comparisons between all the PCIH analogues were then made based on the %SC DNA remaining and the results of the gel quantified by scanning densitometry (Fig. 10). Only results at IBEs of 1 and 3 are shown, as the results at an IBE of 0.1 were all similar to Fe^{II} in the presence of H$_2$O$_2$. Of the HPCIH analogues, HPC3HH was the most damaging in terms of plasmid

degradation, there being no SC DNA remaining at IBEs of 1 and 3 (Fig. 10). Of the remaining analogues, HPCIH, HPC4BBH, HPC4HH, and HPCTH all reduced SC DNA to zero at an IBE of 3. On the other hand, HPCBH, HPC3BBH and HPC2BBH were far less damaging, with greater than 50% of SC DNA remaining at an IBE of 1.

These results were consistent with an earlier DNA degradation study of a smaller subset of the HPCIH analogues.[17] Single or double strand breaks in naked plasmid in this assay were due to Fe-catalysed redox activity and require the complex to be stable in both the divalent and trivalent forms. The ferrous complex of DFO is only formed at very low potential, and as such, it does not participate in Fenton chemistry.[67] Consequently, it shows no significant plasmid degradation activity.[17]

However, redox activity does not necessarily mean that DNA plasmid degradation is inevitable.[17,36] Redox-active Fe complexes that are negatively charged such as $[Fe(EDTA)]^{2-}$ are repelled by like-charged DNA and show no significant plasmid degradation.[17,36] All of the $Fe(PCIH)_2$ analogues degrade naked plasmid to some degree. Interestingly, the most damaging complexes result from ligands that possess potentially H-bond donating substituents (–OH, NH_2; Fig. 10). Ironically, these were also the least active at either mobilising intracellular ^{59}Fe (Fig. 8A) or inhibiting ^{59}Fe uptake from ^{59}Fe-Tf (Fig. 8B). We suggest that these potential H-bond donors promote association of the Fe complex with nucleic acid acceptor sites (phosphate, sugar *etc.*), whereas the analogues with the more hydrophobic groups (phenyl, bromophenyl) do not have a particularly great affinity for DNA.

In terms of the physiological significance of these results, it is important to note that the ability of an Fe-complexed chelator to degrade naked plasmid is only relevant if the complex can enter the nucleus. Previously, we showed[17] that although some of the Fe complexes of the HPCIH analogues were capable of degrading naked plasmid DNA *in vitro*, the damage to nuclear DNA in *intact* human cells was insignificant. This suggests that the $Fe(PCIH)_2$ complexes formed intracellularly do not gain access to DNA in the nuclear compartment.

Conclusions

This investigation represents the first systematic study of the Fe^{II} coordination chemistry of the HPCIH analogues. This work was crucial, as this class of chelator shows great promise as an orally effective drug for the treatment of Fe overload disease.[16,18] A number of important conclusions can be drawn from these experiments. First, unlike most other ligands that have advanced to clinical trials such as DFO, L1 and ICL670A (Fig. 1), the HPCIH analogues are Fe^{II} chelators.

Iron complexes of synthetic chelators may generate potentially cytotoxic free radicals[3] if they participate in redox cycling between the di- and trivalent oxidation states. The aqueous voltammetry of the $Fe(PCIH)_2$ analogues although formally irreversible, involves a reversible chemical reaction (hydration). In any case, the potential at which the $Fe(PCIH)_2$ analogues are oxidised (*ca.* 500 mV *vs.* NHE) means that oxidation to the Fe^{III} state by oxygen will be very slow under physiological conditions. In the presence of strong oxidants such as H_2O_2, oxidation could be more rapid and Fenton chemistry may result. However, whether this leads to nuclear DNA damage or not is debatable and our results so far suggest that the

HPCIH analogues are relatively benign and are well tolerated *in vitro* in cell culture[16,17] and *in vivo* in mice.[18]

The HPCIH analogues show preference for Fe^{II}, forming low-spin bis-ligand Fe^{II} complexes with pM values ranging from 6.1 to 7.1. The variation across the series is relatively small, despite the difference in electronic effect of the distal substituents, ranging from strongly electron-withdrawing, as in the case of the isonicotinoyl group, to strongly electron-donating, as in the case of the 4-aminobenzoyl ring. Also, their Fe^{II} pM values are comparable to the existing drug DFO[43] and the widely investigated H_2PIH.[30,44]

The high $Fe^{III/II}$ redox potentials and instability of the ensuing Fe^{III} complexes effectively rule out compounds of the formula $[Fe(PCIH)_2]^+$ as playing any significant role in a biological context. This means that the HPCIH analogues are incapable of directly competing with Tf for Fe^{III}, whereas DFO is competitive for trivalent Fe.[55] Indeed, the ability of the HPCIH series to prevent Fe uptake from Tf by cells can probably be explained by these chelators acting after Fe release from Tf within the cell.[58] The *in vitro* Fe chelation efficacy of the HPCIH series established in this study is probably attributed to their preference for chelating intracellular Fe^{II}. It is well known that Tf-bound Fe^{III} bound to the transferrin receptor 1 is internalised by receptor-mediated endocytosis.[4] Within the endosome, Fe^{III} is reduced to Fe^{II} and then subsequently transported into the cell by DCT1.[4] This Fe can be used by metabolic processes and incorporation into the iron storage protein, ferritin.[58] Our uptake experiments demonstrate that this Fe^{II} in transit can be intercepted by the HPCIH analogues.

Considering the Fe chelation efficacy of the HPCIH series at both inducing Fe efflux from pre-labelled cells and preventing Fe uptake from Tf, the most active chelators were HPCBH and HPCTH. The reasons for this high activity relative to the other HPCIH chelators may be related to an optimal lipophilic balance between the ligand and Fe complex. Certainly, in the current study, it was clear that highly hydrophilic substituents such as the amino and hydroxyl group did not confer high activity and resulted in compounds which could degrade DNA. Hence, in terms of structure–activity relationships, these latter groups should be avoided in the design of future ligands.

In summary, the HPCIH analogues are an emerging class of Fe chelators that have already been found to be orally-active and well tolerated in a mouse model.[18] The present study has shown that these ligands are specifically Fe^{II} chelators (not Fe^{III}). Considering this, rather than competing with other more effective Fe^{III} binding proteins such as Tf, the HPCIH analogues must target divalent Fe within the cell *e.g.* the labile Fe pool. The more hydrophobic chelators of the series are most effective in terms of their ability to mobilise ^{59}Fe from ^{59}Fe-loaded cells and to prevent cellular uptake from ^{59}Fe-Tf. It is also these lipophilic analogues that show the least activity in degrading plasmid DNA, which is also an important property of a clinically effective chelator for the treatment of Fe overload disease.

Acknowledgements

References

1 D. S. Kalinowski and D. R. Richardson, *Pharmacol. Rev*, 2005, **57**, 547–583.

2 M. T. Nunez, M. A. Garate, M. Arredondo, V. Tapia and P. Munoz, *Biol. Res.*, 2000, **33**, 133–142.

3 H. B. Dunford, *Coord. Chem. Rev.*, 2002, **233**, 311–318.

4 N. C. Andrews, *New Engl. J. Med.*, 1999, **341**, 1986–1995.

5 P. Ponka, in Development of Iron Chelators for Clinical Use, ed. R. J. Bergeron and G. M. Brittenham, CRC Press, 1994, pp. 1–32.

6 S. T. Callender and D. J. Weatherall, *Lancet*, 1980, **2**, 689.

7 D. Richardson, P. Ponka and E. Baker, *Cancer Res.*, 1994, **54**, 685–689.

8 N. F. Olivieri and G. M. Brittenham, *Blood*, 1997, **89**, 739–761.

9 P. Ponka, J. Borova, J. Neuwirt and O. Fuchs, *FEBS Lett.*, 1979, **97**, 317–321.

10 P. Ponka, R. W. Grady, A. Wilczynska and H. M. Schulman, *Biochim. Biophys. Acta*, 1984, **802**, 477–489.

11 D. R. Richardson, C. Mouralian, P. Ponka and E. Becker, *Biochim. Biophys. Acta*, 2001, **1536**, 133–140.

12 D. R. Richardson, *J. Lab. Clin. Med.*, 2001, **137**, 324–329.

13 A. R. Cohen, *Hematology*, 2006, 42–47.

14 E. Nisbet-Brown, N. F. Olivieri, P. J. Giardina, R. W. Grady, E. J. Neufeld, R. Sechaud, A. J. Krebs-Brown, J. R. Anderson, D. Alberti, K. C. Sizer and D. G. Nathan, *Lancet*, 2003, **361**, 1597–1602.

15 J. M. Donavan, M. Plone, R. Dagher, M. Bree and J. Marquis, *Ann. N. Y. Acad. Sci.*, 2005, **1054**, 492–494.

16 E. Becker and D. R. Richardson, *J. Lab. Clin. Med.*, 1999, **134**, 510–521.

17 T. B. Chaston and D. R. Richardson, *JBIC, J. Biol. Inorg. Chem.*, 2003, **8**, 427–438.

18 C. S. M. Wong, J. C. Kwok and D. R. Richardson, *Biochim. Biophys. Acta*, 2004, **1739**, 70–80.

19 C. M. Armstrong, P. V. Bernhardt, P. Chin and D. R. Richardson, *Eur. J. Inorg. Chem.*, 2003, 1145–1156.

20 P. V. Bernhardt, P. Chin and D. R. Richardson, *JBIC, J. Biol. Inorg. Chem.*, 2001, **6**, 801–809.

21 P. Gans, A. Sabatini and A. Vacca, *J. Chem. Soc., Dalton Trans.*, 1985, 1195–1200.

22 L. J. Farrugia, *J. Appl. Crystallogr.*, 1999, **32**, 837–838.

23 G. M. Sheldrick, *SHELXL-97-A Program for Crystal Structure Refinement*, University of Göttingen, Germany, 1997 Release 97–2.

24 L. J. Farrugia, *J. Appl. Crystallogr.*, 1997, **30**, 565.

25 D. R. Richardson, E. H. Tran and P. Ponka, *Blood*, 1995, **86**, 4295–4306.

26 D. R. Richardson and E. Baker, *Biochim. Biophys. Acta*, 1990, **1053**, 1–12.

27 D. R. Richardson and P. Ponka, *J. Lab. Clin. Med.*, 1994, **124**, 660–671.

28 D. R. Richardson and K. Milnes, *Blood*, 1997, **89**, 3025–3038.

29 D. R. Richardson, E. Becker and P. V. Bernhardt, *Acta Crystallogr., Sect. C*, 1999, **C55**, 2102–2105.

30 D. R. Richardson, L. M. W. Vitolo, G. T. Hefter, P. M. May, B. W. Clare, J. Webb and P. Wilairat, *Inorg. Chim. Acta*, 1990, **170**, 165–170.

31 M. Garcia-Vargas, M. Belizon, M. P. Hernandez-Artiga, C. Martinez and J. A. Perez-Bustamante, *Appl. Spectrosc.*, 1986, **40**, 1058–1062.

32 J. E. Dubois, H. Fakhrayan, J. P. Doucet and J. M. E. Chahine, *Inorg. Chem.*, 1992, **31**, 853–859.

33 N. J. Lees-Gayed, M. A. Abou-Taleb, I. A. El-Bitash and M. F. Iskander, *J. Chem. Soc., Perkin Trans. 2*, 1992, 213–217.

34 P. Doungdee, S. Sarel, I. Ringel, D. Gibson, N. Wongvisetsirikul and S. Avramovicigrisaru, *Heterocycles*, 1995, **40**, 241–248.

35 P. Doungdee, S. Sarel, N. Wongvisetsirikul and S. Avramovicigrisaru, *J. Chem. Soc., Perkin Trans. 2*, 1995, 319–323.

36 P. V. Bernhardt, L. M. Caldwell, T. B. Chaston, P. Chin and D. R. Richardson, *JBIC, J. Biol. Inorg. Chem.*, 2003, **8**, 866–880.

37 P. V. Bernhardt, P. Chin and D. R. Richardson, *Dalton Trans.*, 2004, 3342–3346.

38 R. M. Silverstein, G. C. Basslerand T. C. Morrill, *Spectrometric Identification of Organic Compounds*, John Wiley & Sons, Inc., Singapore, 1981.

39 D. H. Williams, I. Fleming, *Spectroscopic Methods in Organic Chemistry*, McGraw-Hill Book Company, London, 1987.

40 A. T. Florence and D. Attwood, *Physiochemical Principles of Pharmacy*, Macmillan, London, 1988.

41 W. R. Harris, K. N. Raymond and F. L. Weitl, *J. Am. Chem. Soc.*, 1981, **103**, 2667–2675.

42 J. R. Telford and K. N. Raymond, in *Comprehensive Supramolecular Chemistry*, ed. J. M. Lehn, J. L. Atwood, J. E. D. Davies, D. D. Macnicol, F. Vogtle and G. W. Gokel, Pergamon, 1996, vol. 1, pp. 245–266.

43 A. E. Martell, R. M. Smith and R. J. Motekaitis, *Critically Selected Stability Constants of Metal Complexes Database*, Texas A&M University, 1997.

44 L. M. Wis Vitolo, G. T. Hefter, B. W. Clare and J. Webb, *Inorg. Chim. Acta*, 1990, **170**, 171–176.

45 H. Keberle, *Ann. N. Y. Acad. Sci.*, 1964, **119**, 758.

46 S. Dhungana, P. S. White and A. L. Crumbliss, *JBIC, J. Biol. Inorg. Chem.*, 2001, **6**, 810–818.

47 C. Hansch, *Acc. Chem. Res.*, 1969, **2**, 232–239.

48 J. T. Edward, P. Ponka and D. R. Richardson, *Biometals*, 1995, **8**, 209–217.

49 J. T. Edward, *Biometals*, 1998, **11**, 203–205.

50 B. L. Rai, L. S. Dekhordi, H. Khodr, Y. Jin, Z. D. Liu and R. C. Hider, *J. Med. Chem.*, 1998, **41**, 3347–3359.

51 F. Thomas, P. Baret, D. Imbert, J. L. Pierre and G. Serratrice, *Bioorg. Med. Chem. Lett.*, 1999, **9**, 3035–3040.

52 P. V. Bernhardt, P. Chin, P. C. Sharpe, J.-Y. C. Wang and D. R. Richardson, *JBIC, J. Biol. Inorg. Chem.*, 2005, **10**, 761–777.

53 C. Hansch and E. J. Lien, *J. Med. Chem.*, 1971, **14**, 653–670.

54 J. T. Edward, F. L. Chubb and J. Sangster, *Can. J. Physiol. Pharmacol.*, 1997, **75**, 1362–1368.

55 E. Baker, D. Richardson, S. Gross and P. Ponka, *Hepatology*, 1992, **15**, 492–501.

56 D. B. Lovejoy and D. R. Richardson, *Blood*, 2002, **100**, 666–676.

57 G. Darnell and D. R. Richardson, *Blood*, 1999, **94**, 781–792.

58 D. R. Richardson and P. Ponka, *Biochim. Biophys. Acta*, 1997, **1331**, 1–40.

59 T. G. St Pierre, D. R. Richardson, E. Baker and J. Webb, *Biochim. Biophys. Acta*, 1992, 1135, 154-158.

60 D. R. Richardson and P. Ponka, *J. Lab. Clin. Med.*, 1998, **131**, 306–315.

61 T. B. Chaston and D. R. Richardson, *Am. J. Hematol.*, 2003, **73**, 200–210.

62 K. W. Kohn, *Pharmacol. Ther.*, 1991, **49**, 55–77.

63 D. R. Lloyd, D. H. Phillips and P. L. Carmichael, *Chem. Res. Toxicol.*, 1997, **10**, 393–400.

64 D. R. Lloyd, P. L. Carmichael and D. H. Phillips, *Chem. Res. Toxicol.*, 1998, **11**, 420–427.

65 M. Hermes-Lima, E. Nagy, P. Ponka and H. M. Schulman, *Free Radical Biol. Med.*, 1998, **25**, 875–880.

66 A. C. Mello and R. Meneghini, *Biochim. Biophys. Acta*, 1984, **781**, 56–63.

67 I. Spasojevic, S. K. Armstrong, T. J. Brickman and A. L. Crumbliss, *Inorg. Chem.*, 1999, **38**, 449–454.